

Spectral form factor and power spectrum for trapped rotating interacting bosons: An exact diagonalization study

Mohd Talib ^{*} and M. A. H. Ahsan [†]

Department of Physics, Jamia Millia Islamia (A Central University), New Delhi, 110025, India.

(Dated: December 2, 2025)

We present an exact diagonalization study of the spectral form factor and the power spectrum for externally impressed rotating bosons in a quasi-two-dimensional harmonic trap interacting via repulsive Gaussian potential. Our focus is on the spectral correlations arising from the condensate depletion as a result of the formation of quantized vortices and the strong interaction, which leads to chaos in the system. We consider two distinct interaction regimes: moderate, where the interaction energy is small compared to the trap energy, and strong, where it is comparable. For the non-rotating case, the spectral form factor (SFF) in the moderate interaction regime exhibits a dip-plateau structure characteristic of integrable systems, while in the strong interaction regime it develops a weak ramp, signalling a transition to pseudo-integrable behavior. For the rotating single-vortex state, the SFF in the moderate interaction regime shows the onset of a weak ramp consistent with pseudo-integrability, whereas in the strong interaction regime the ramp becomes significantly more pronounced, indicating strongly chaotic behavior. For the multi-vortex states in the strong interacting regime, the SFF exhibits a clear dip-ramp-plateau structure, indicative of chaotic behavior. The corresponding power spectrum results further corroborate these findings: integrable system exhibits the characteristic $1/f^\alpha$ (with $\alpha \approx 2$) noise, chaotic system shows the ubiquitous $1/f^\alpha$ (with $\alpha \approx 1$) noise, and pseudo-integrable system yields intermediate exponents with $1 < \alpha < 2$.

I. INTRODUCTION

A precise and universally accepted definition of quantum chaos has yet to be established. Two key conjectures that link quantum chaos to random matrix theory (RMT) are the Berry-Tabor conjecture [1] and the Bohigas-Giannoni-Schmit (BGS) conjecture [2]. The Berry-Tabor conjecture asserts that quantum systems whose classical counterparts are integrable exhibit Poissonian level statistics in their energy spectra. The BGS conjecture postulates that the level statistics of quantum systems with classically chaotic dynamics follow one of the random matrix ensembles, determined by the symmetry properties of the Hamiltonian. Specifically, systems that are time-reversal invariant and possess rotational symmetry, allowing the Hamiltonian to be represented as a real symmetric matrix, correspond to the Gaussian Orthogonal Ensemble (GOE). Systems without time-reversal invariance, for which the Hamiltonian is complex Hermitian, correspond to the Gaussian Unitary Ensemble (GUE). Meanwhile, systems with half-integer spin that are time-reversal invariant but lack rotational symmetry are described by the Gaussian Symplectic Ensemble (GSE) [3, 4]. These conjectures are strongly supported by extensive theoretical and numerical studies, making them foundational principles in the field of quantum chaos.

In our recent study, we investigated the statistical properties of the lowest 100 energy levels of harmonically confined interacting bosons using both short- and long-range correlation measures [5]. Our study revealed a subtle interplay between interaction energy and the trapping potential in shaping the level statistics, along with an enhancement of chaotic behavior induced by rotation. In the present work,

we focus on the late-time behavior of the system through the spectral form factor (SFF), which has been widely employed in studies of many-body quantum chaos [6–9], sparse Sachdev-Ye-Kitaev model [10, 11], black holes [12–15], and many-body localization [16–18], and was recently measured experimentally in quantum processors [19]. To date, the SFF has not been explored in trapped rotating interacting bosons. Unlike traditional spectral measures, such as the nearest-neighbor spacing distribution, Dyson-Mehta Δ_3 statistic, or level number variance $\Sigma^2(L)$, the SFF captures both short- and long-range spectral correlations. It typically exhibits three characteristic regimes: the slope, ramp, and plateau. The slope corresponds to early-time dynamics, while the ramp reflects level repulsion and serves as a hallmark of quantum chaos. At late times, the ramp saturates, giving rise to a plateau, which corresponds to strong eigenvalue repulsion when energy differences approach the mean level spacing.

The power spectrum provides an additional statistical approach to examine both short-range and long-range correlations. Its relevance to quantum chaos was first investigated nearly two decades ago through a series of studies [20–24]. The utility of the power spectrum has been firmly established in studies of quantum chaos across diverse systems including the quartic oscillator and the kicked top [25], and recently in molecular resonances of erbium isotopes [26], yet its application to trapped rotating interacting bosons remains largely unexplored. The behavior of the power spectrum forms a diagnostic of integrability and chaos: integrable systems are associated with a $1/f^2$ noise, while chaotic systems exhibit a $1/f$ noise dependence. For pseudo-integrable regimes, the power-law exponent α takes values between $1 < \alpha < 2$, signifying a crossover between the two limiting cases.

The objective of this work is to explore the onset of quantum chaos in a system of interacting bosons confined in a harmonic trap, using the spectral form factor and the power spectrum as diagnostic tools. The Bose-Einstein con-

^{*} rs.mtalib@jmi.ac.in

[†] mahsan@jmi.ac.in

condensation (BEC) refers to the phenomenon in which macroscopically large number of bosons of order $O(N)$ occupy the same single-particle quantum state [27]. In the context of BEC in weakly interacting Bose gas [28], it is well established that, in the absence of rotation with total angular momentum $L_z = 0$, an increase in the interaction strength causes particles to scatter from the single-particle angular momentum quantum state with $m = 0$ to higher energy single-particle states with $m \neq 0$, leading to depletion of the condensate [28]. When the condensate is subjected to an externally impressed rotation, the condensate acquires quantized angular momentum $L_z = N$ through the formation of single-vortex state, resulting in the macroscopic occupation of single-particle angular momentum state with $m = 1$ and so on for the higher quantized total angular momentum multi-vortex states. The emergence of these quantized vortex states further enhances the transfer of particles out of the condensate, thus causing an even larger depletion of the condensate as compared to the non-rotating case [29, 30]. The condensate depletion caused by quantized vortex formation and strong interparticle interactions [31, 32] enhances spectral correlations and drives the system toward chaotic behavior. Although these effects are well studied in superfluidity, their direct impact on spectral correlations and hence the integrable-chaotic transition remains unexplored. Here, we address this issue by connecting condensate depletion to the strengthening of spectral correlations and the resulting onset of quantum chaos.

The rest of the paper is organized in the following manner. Sec. II introduces the model Hamiltonian for harmonically trapped interacting bosons. Sec. III outlines the diagnostic tools of quantum chaos employed in this study, particularly the spectral form factor and the power spectrum. In Sec. IV, we present and discuss the numerical results, and Sec. V concludes with a summary of the main findings.

II. THE MODEL HAMILTONIAN

We consider a system of N interacting bosons confined in a cylindrically symmetric harmonic trap with anisotropy parameter $\lambda_z \equiv \omega_z/\omega_\perp$. The Hamiltonian and the total angular momentum in the laboratory frame are given by

$$\begin{aligned} \hat{H}^{\text{lab}} = & \sum_{i=1}^N \left[\frac{1}{2M} \left(\frac{\hbar}{i} \nabla_{\perp i} \right)^2 + \frac{1}{2} M \omega_\perp^2 r_{\perp i}^2 \right] \\ & + \sum_{i=1}^N \left[\frac{1}{2M} \left(\frac{\hbar}{i} \nabla_{z_i} \right)^2 + \frac{1}{2} M \omega_z^2 z_i^2 \right] \\ & + \frac{1}{2} \frac{4\pi\hbar^2 a_{sc}}{M} \left(\frac{1}{\sqrt{2\pi}\sigma} \right)^3 \\ & \times \sum_{i \neq j}^N \exp \left[-\frac{(r_{\perp i} - r_{\perp j})^2 + (z_i - z_j)^2}{2\sigma^2} \right] \quad (1) \\ \hat{L}_z^{\text{lab}} = & \frac{\hbar}{i} \sum_{i=1}^N (\mathbf{r}_i \times \nabla_i)_z, \end{aligned}$$

where M is the mass of the boson, ω_\perp and ω_z are the radial and the axial trapping frequencies, respectively. The first term in Eq. (1) represents the kinetic energy and the harmonic confinement in the xy-plane, while the second term corresponds to the kinetic energy and the harmonic confinement along the z-direction. The third term in Eq. (1) represents the two-body interaction between the particles modeled by a finite-range Gaussian potential with width σ and a_{sc} denotes the s-wave scattering length for interparticle collisions that can be experimentally tuned via Feshbach resonances [33, 34]. In this work, we restrict to the repulsive regime by assuming $a_{sc} > 0$.

Further, the system is subjected to an externally impressed rotational velocity Ω about the z-axis. The Hamiltonian for the system in the co-rotating frame is given by [28]

$$\hat{H}^{\text{rot}} = \hat{H}^{\text{lab}} - \Omega \hat{L}_z^{\text{lab}},$$

where Ω serves as the Lagrange multiplier to constrain the system in a given total angular momentum state \hat{L}_z^{lab} .

For $\lambda_z \gg 1$, the particles are effectively constrained to move in the xy-plane and there will be no excitation along the z-direction. The effective Hamiltonian in xy-plane obtained by tracing out the z-degree of freedom, as in Eq. (A4) with $n_z = 0$, is given by

$$\begin{aligned} \hat{H}' = & \sum_{i=1}^N \left[\frac{1}{2M} \left(\frac{\hbar}{i} \nabla_{\perp i} \right)^2 + \frac{1}{2} M \omega_\perp^2 r_{\perp i}^2 \right] + \frac{1}{2} \hbar \omega_z \\ & + \underbrace{\frac{4\pi\hbar^2 a_{sc}}{M} \frac{1}{\sqrt{2\pi}} \sqrt{\frac{\lambda_z}{a_\perp^2 \left[1 + \left(\frac{\sigma}{a_\perp} \right)^2 \lambda_z \right]}}}_{g'_2} \\ & \times \left(\frac{1}{\sqrt{2\pi}\sigma} \right)^2 \sum_{i \neq j}^N \exp \left[-\frac{(r_{\perp i} - r_{\perp j})^2}{2\sigma^2} \right], \quad (2) \end{aligned}$$

where g'_2 is the effective two-body interaction strength in xy-plane and has the dimension of [energy \times area]. In the limit of the interaction range being small compared to the trap length i.e. $\frac{\sigma}{a_\perp} \ll 1$, g'_2 reduces to

$$g'_2 \approx \frac{4\pi\hbar^2 a_{sc}}{M a_\perp} \sqrt{\frac{\lambda_z}{2\pi}}.$$

The dimensionless effective Hamiltonian in xy-plane defined as $\hat{H} \equiv \frac{1}{\hbar\omega_\perp} \hat{H}' - \frac{1}{2} \lambda_z$, with $a_\perp = \sqrt{\frac{\hbar}{M\omega_\perp}}$, is thus given by

$$\begin{aligned} \hat{H} = & \sum_{i=1}^N \left[\frac{1}{2} \left(\frac{a_\perp \nabla_{\perp i}}{i} \right)^2 + \frac{1}{2} \left(\frac{r_{\perp i}}{a_\perp} \right)^2 \right] \\ & + g_2 \left(\frac{a_\perp}{\sqrt{2\pi}\sigma} \right)^2 \sum_{i \neq j}^N \exp \left[-\frac{(r_{\perp i} - r_{\perp j})^2}{2\sigma^2} \right], \quad (3) \end{aligned}$$

where

$$g_2 \approx \frac{4\pi a_{sc}}{a_\perp} \sqrt{\frac{\lambda_z}{2\pi}}. \quad (4)$$

The Hamiltonian in Eq. (3) is iteratively diagonalized using Davidson algorithm [35] to obtain the variationally exact low-lying energy eigenvalues and the corresponding eigenvectors as described in [28]. With the lowest 100 energy levels, we proceed to examine the effect of both vortex-induced and interaction-driven depletion of the condensate, leading to chaotic behavior in the system, as discussed in the following.

III. DIAGNOSTIC TOOLS OF QUANTUM CHAOS

The statistical tools employed in our analysis to probe the late-time behavior and the short- as well as the long-range correlations in the system are outlined below.

A. Spectral Form Factor

The spectral form factor (SFF) for a system with L number of energy levels $\{\epsilon_i | i = 1, 2, \dots, L\}$ is defined as [36–39]

$$\langle K(\tau) \rangle = \left\langle \frac{|Z(i\tau)|^2}{|Z(0)|^2} \right\rangle = \frac{1}{L^2} \left\langle \sum_{i,j} \exp[-i(\epsilon_i - \epsilon_j)\tau] \right\rangle, \quad (5)$$

where $Z(i\tau)$ is the partition function defined as

$$Z(i\tau) = \text{Tr} (e^{-iH\tau}) = \sum_{i=1}^L e^{-i\epsilon_i \tau}.$$

The SFF is known to be a non-self-averaging quantity [40], meaning that its value can fluctuate significantly between different realizations of the spectrum. As a result, appropriate averaging procedures are required to extract universal features. In this study, we apply a moving time average within a logarithmic window [8] to make the ramp behavior more apparent.

For small values of $r \equiv |\epsilon_1 - \epsilon_2|$ in units of unfolded mean level spacings, the two-level cluster function can be expanded as [36]

$$Y_2(r) = 1 - \frac{\pi^2}{6}r + \frac{\pi^4}{60}r^3 - \frac{\pi^4}{135}r^4 + \dots \quad (6)$$

whereas for large r , it takes the asymptotic form

$$Y_2(r) = \frac{1}{\pi^2 r^2} - \frac{1 + \cos^2(\pi r)}{\pi^4 r^4} + \dots, \quad (7)$$

The two-level form factor $b(\tau)$ is defined as the Fourier transform of $Y_2(r)$:

$$b(\tau) = \int_{-\infty}^{\infty} Y_2(r) e^{2\pi i \tau r} dr. \quad (8)$$

The corresponding explicit expressions are given by

$$b(\tau) = \begin{cases} 1 - 2|\tau| + |\tau| \ln(1 + 2|\tau|), & |\tau| \leq 1, \\ -1 + |\tau| \ln\left(\frac{2|\tau| + 1}{2|\tau| - 1}\right), & |\tau| \geq 1. \end{cases}$$

The analytical expression for the spectral form factor (SFF) in the Gaussian Orthogonal Ensemble (GOE) is obtained as

$$K^{\text{GOE}}(\tau) = 1 - b(\tau), \quad (9)$$

which simplifies to

$$K^{\text{GOE}}(\tau) = \begin{cases} 2\tau - \tau \ln(1 + 2\tau), & \tau \leq 1, \\ 2 - \tau \ln\left(\frac{2\tau + 1}{2\tau - 1}\right), & \tau \geq 1, \end{cases} \quad (10)$$

where τ is in the units of Heisenberg time τ_H i.e $\tau = \frac{t}{\tau_H}$.

The dip time and the Heisenberg time

The SFF allows one to extract two important characteristic time scales of the system, namely, the dip time τ_{dip} and the Heisenberg time τ_H . The dip time τ_{dip} denotes the time at which the SFF reaches its minimum value after the initial stage of oscillatory decay. This time scale signals the transition from the short-time regime—dominated by nonuniversal features and rapid fluctuations—to the onset of the linear ramp, where correlations between energy levels begin to develop and the behaviour of the SFF starts to reflect universal random-matrix predictions. In contrast, the Heisenberg time τ_H corresponds to the point at which the linear ramp terminates and the SFF saturates to a plateau. This saturation marks the regime where the system has fully resolved the discrete nature of its spectrum, indicating that long-range spectral correlations have become fully established. The Heisenberg time τ_H serves as the boundary between the linear ramp regime and the long-time plateau region, where the SFF remains constant due to the finite size of the spectrum.

B. Power Spectrum

The power spectrum effectively quantifies the deviation of the unfolded excitation energies from their mean value. In a quantum system, the fluctuations of the energy-level spacings $s_i = \epsilon_{i+1} - \epsilon_i$ about their mean value $\langle s \rangle$ defined as

$$\delta_n = \sum_{i=1}^n (s_i - \langle s \rangle), \quad (11)$$

can be treated as discrete time series [20–22, 41]. The Fourier transform of this series defined as

$$\hat{\delta}_k = \frac{1}{\sqrt{L}} \sum_{n=1}^n \delta_n e^{-\frac{2\pi i k n}{L}}, \quad (12)$$

and the corresponding power spectrum given by

$$P_k = |\hat{\delta}_k|^2, \quad (13)$$

provides a means of distinguishing transition from regular to chaotic behavior [42].

For chaotic systems, $P_k \propto \frac{1}{k}$, whereas integrable systems follow $P_k \propto \frac{1}{k^2}$. This behavior holds regardless of whether time-reversal invariance is maintained, meaning it is independent of the universality class.

IV. RESULTS & DISCUSSIONS

We present our study on a system of $N = 12, 16$, and 20 bosonic atoms of ^{87}Rb confined in a quasi-two-dimensional harmonic trap and interacting via repulsive two-body potential Gaussian in particle-particle separation. The system parameters are chosen as in references [43, 44] with trap anisotropy parameter $\lambda_z = \frac{\omega_z}{\omega_\perp} = 4$ and the axial frequency of the trap $\omega_z = 2\pi \times 220$ Hz. This choice with mass M of the ^{87}Rb atom yields a radial trap length of $a_\perp = \sqrt{\frac{\hbar}{M\omega_\perp}} = 1.446 \mu\text{m}$. The interaction range of the Gaussian potential is fixed at $\sigma = 0.1 a_\perp$. The effective interaction strength in the mean-field approximation for a contact potential is characterized by the parameter $\frac{Na_{sc}}{a_\perp}$ [45], where N is the number of bosonic atoms and a_{sc} the s -wave atom-atom scattering length. We employ exact diagonalization method which restricts the system size to a few tens of particles due to the exponential increase of the many-body Hilbert space with the number of particles N . To achieve values of the parameter Na_{sc}/a_\perp relevant to experimental conditions, we parametrically vary the s -wave scattering length. With $a_0 = 0.05292$ nm as the Bohr radius, we set $a_{sc} = 1000 a_0$ to represent the moderately interacting regime, where the interaction energy remains small compared to the trap energy, and $a_{sc} = 10000 a_0$ to represent the strongly interacting regime, where the interaction energy becomes comparable to the trap energy. With these parameters, the dimensionless interaction strength for the quasi-2D system, given by $g_2 \approx \frac{4\pi a_{sc}}{a_\perp} \sqrt{\frac{\lambda_z}{2\pi}}$ takes the values $g_2 = 0.3669$ in the moderate interaction regime and $g_2 = 3.669$ in the strong interaction regime.

We now present our numerical results for the spectral form factor and the power spectrum for different number of bosons, considering both the non-rotating and the rotating single-vortex states in the moderate and the strong interaction regimes. We also study the multi-vortex states ($L_z = 2N$ and $L_z = 3N$) in the strong interaction regime.

A. Non-rotating case

In the following we consider the non-rotating case in both the moderate and the strong interaction regimes.

1. Moderate interaction regime

The SFF for $N = 12, 16$ and 20 bosons is presented in the upper panel of Fig. 1. The spectral form factor (SFF)

exhibits an initial oscillatory decay at early times. As time progresses, the oscillations diminish and the SFF reaches a pronounced minimum, commonly referred to as the dip time. Beyond this point, and particularly for times longer than the Heisenberg time, the SFF no longer decreases; instead, it settles into a constant long-time value. This long-time saturation is a key indicator of the underlying spectral properties of the system. In fully chaotic quantum systems, one typically observes a linear ramp in the SFF after the dip time, which reflects the presence of spectral correlations and hence the level repulsion and the spectral rigidity predicted by RMT. However, in the present case, such a linear ramp is absent. As illustrated in the upper panel of Fig. 1, the SFF fails to develop the characteristic linear ramp-like growth. This deviation from chaotic behavior implies that the system does not exhibit the level repulsion expected from RMT. The absence of the ramp therefore signals that the system resides in an integrable regime, where the energy levels are only weakly correlated. Instead of showing the universal correlations typical of chaotic spectra, the level statistics more closely resemble those of uncorrelated or Poissonian spectra. This integrable behavior can be traced back to the physical structure of the system: a large condensate fraction is present in this regime. When a significant number of the particles occupy the ground state, the excitation spectrum becomes sparse and interactions among excited levels are weak. As a result, spectral correlations are suppressed, leading to the observed saturation in the SFF and the lack of RMT-like features. The power spectrum $P(k)$ for different number of bosons is shown in the left panel of Fig. 2. The value of the power-law exponent α , obtained from a linear fit to the data, is found to be close to 2. This indicates that, in the moderate interaction regime, the system follows Poisson statistics, which is characteristic of integrable behavior.

2. Strong interaction regime

The SFF and power spectrum in the strong interaction regime are presented in Fig. 1 (lower panel) and Fig. 2 (right panel), respectively. The SFF displays the characteristic dip-ramp-plateau structure, as illustrated in Fig. 1 (lower panel). At early times, the SFF decreases and reaches a minimum at the dip time. Beyond this dip, a slight but noticeable linear increase—the ramp—begins to develop. Although this ramp is not as pronounced as in fully chaotic systems, its presence is significant: it marks the emergence of weak spectral correlations among the energy levels. As time continues to evolve, the SFF eventually saturates to a constant long-time value, forming the plateau. This long-time saturation reflects the fact that the system has entered a regime where some degree of level repulsion and spectral rigidity has begun to appear, although not to the extent predicted by RMT for strongly chaotic systems. The appearance of a small ramp followed by a plateau therefore signals the onset of weak chaos in the spectrum. The physical origin of this behavior lies in the interaction-driven depletion of the condensate at strong coupling. As the interaction strength increases, a non-negligible number of particles are scattered to excited

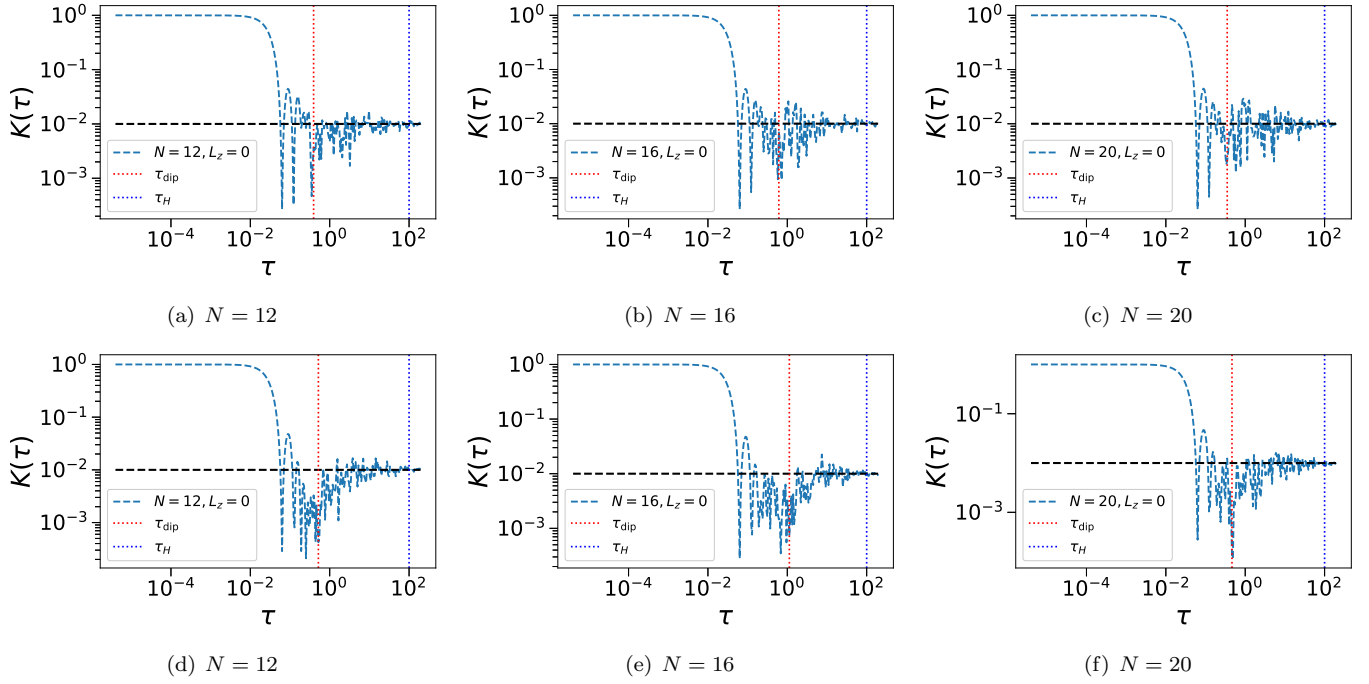


FIG. 1. (Color online) Spectral form factor $K(\tau)$ (with moving time average in a logarithmic window) on the log-log scale in the moderate interaction regime with $g_2 = 0.3669$ (upper panel) and the strong interaction regime with $g_2 = 3.669$ (lower panel) for $N = 12, 16$ and 20 bosons with total angular momentum $L_z = 0$. The horizontal dashed line corresponds to the asymptotic limit of the SFF, $\langle K(\tau) \rangle = 1/L$, with L denoting the total number of energy levels considered. The orange dotted vertical lines mark the dip time τ_{dip} and the blue dotted vertical lines mark the Heisenberg time τ_H .

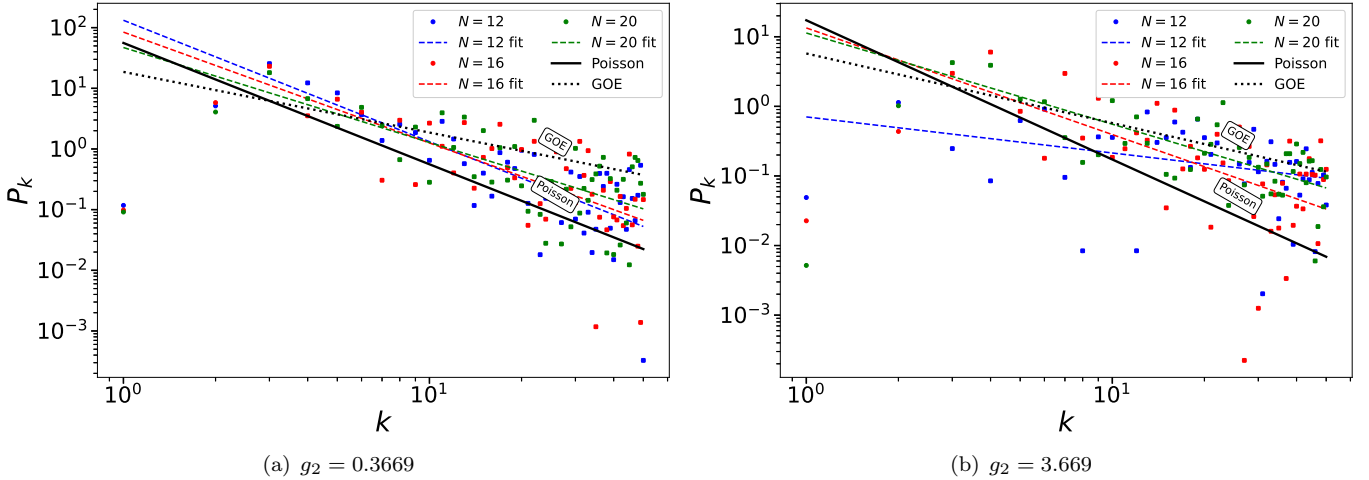


FIG. 2. (Color online) Plot of the power spectrum P_k vs k on the log-log scale in the moderate (left) and the strong (right) interaction regimes for $N = 12, 16$ and 20 bosons with total angular momentum $L_z = 0$. The dots are our numerical results of $N = 12, 16$ and 20 bosons. The blue dashed, the red dashed and the green dashed lines are the straight line fits for $N = 12, 16$ and 20 bosons, respectively. The black square line and the black solid line are the reference lines for the GOE and the Poisson statistics, respectively.

states, due to which the condensate fraction decreases [46]. This scattering of particles from the ground state to the excited states enhances the coupling among different many-body configurations, leading to a partial breakdown of integrability. Consequently, weak spectral correlations emerge, which manifest in the SFF as the small linear ramp and subsequent plateau observed in the numerical results. For number of bosons, the fitted lines to the numerical data closely follow the GOE trend, with power-law exponents

lying in the range $1 < \alpha < 2$, suggesting that the system enters a pseudo-integrable regime.

B. Rotating single-vortex ($L_z = N$) state

In the following we consider the rotating single-vortex $L_z = N$ state in both the moderate and the strong interaction regimes.

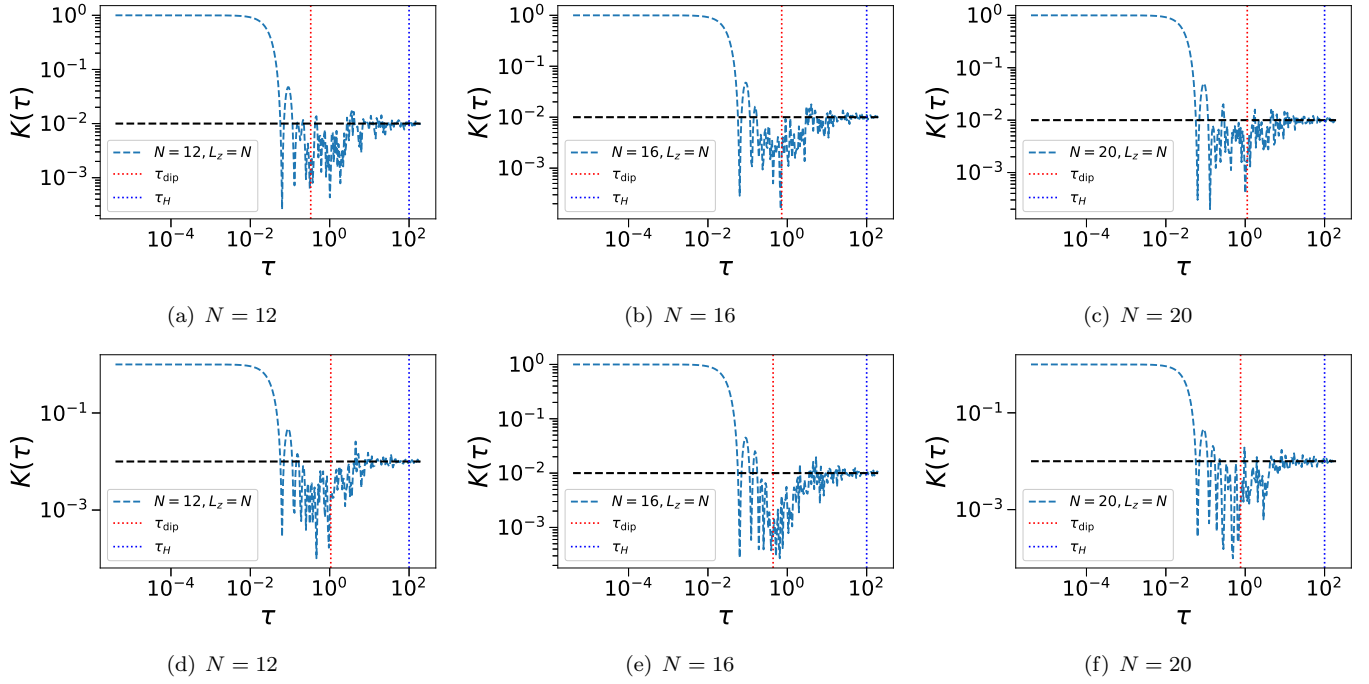


FIG. 3. (Color online) Spectral form factor $K(\tau)$ (with moving time average in a logarithmic window) on the log-log scale in the moderate interaction regime with $g_2 = 0.3669$ (upper panel) and the strong interaction regime with $g_2 = 3.669$ (lower panel) for $N = 12, 16$ and 20 bosons with total angular momentum $L_z = N$. The horizontal dashed line corresponds to the asymptotic limit of the SFF, $\langle K(\tau) \rangle = 1/L$, with L denoting the total number of energy levels considered. The orange dotted vertical lines mark the dip time τ_{dip} and the blue dotted vertical lines mark the Heisenberg time τ_H .

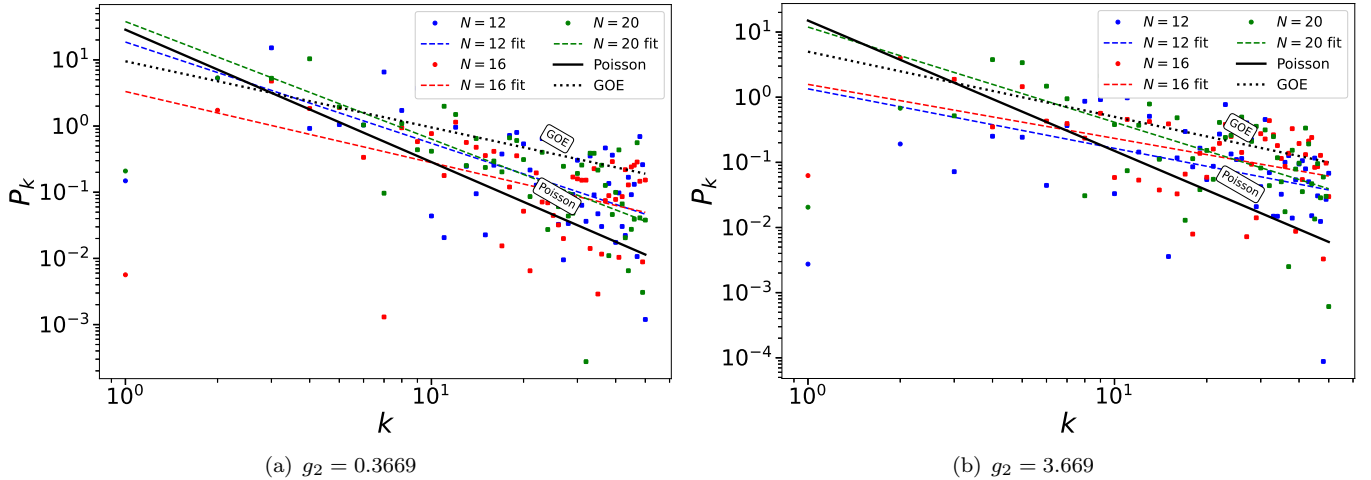


FIG. 4. (Color online) Plot of the power spectrum P_k vs k on the log-log scale in the moderate (left) and the strong (right) interaction regimes for $N = 12, 16$ and 20 bosons with total angular momentum $L_z = N$. The dots are our numerical results of $N = 12, 16$ and 20 bosons. The blue dashed, the red dashed and the green dashed lines are the straight line fits for $N = 12, 16$ and 20 bosons, respectively. The black square line and the black solid line are the reference lines for the GOE and the Poisson statistics, respectively.

1. Moderate interaction regime

The SFF and power spectrum corresponding to the rotating single-vortex state ($L_z = N$) in the moderate interaction regime are presented in Fig. 3 (upper panel) and Fig. 4 (left panel), respectively. In the absence of rotation, the system retains its integrable character, and the energy levels exhibit only weak correlations. However,

when a quantized vortex is formed, the situation changes significantly. The formation of the vortex modifies the structure of the condensate by imposing a phase winding, which in turn perturbs the single-particle states of the system. This perturbation promotes scattering of particles out of the macroscopically occupied ground state and into higher single-particle modes, leading to a noticeable depletion of the BEC. As particles are redistributed among excited states, the coupling between different many-body

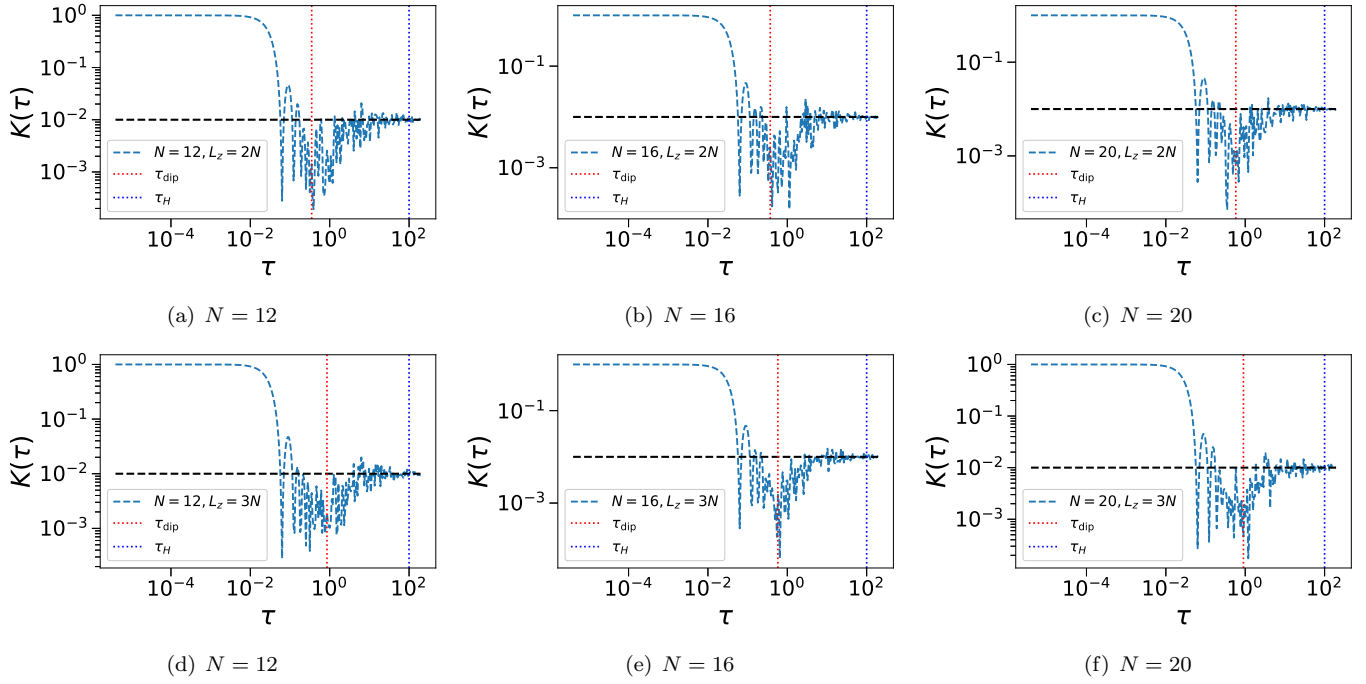


FIG. 5. (Color online) Spectral form factor $K(\tau)$ (with moving time average in a logarithmic window) on the log-log scale in the strong interaction regime with $g_2 = 3.669$ for $N = 12, 16$ and 20 bosons with total angular momentum $L_z = 2N$ (upper panel) and $L_z = 3N$ (lower panel). The horizontal dashed line corresponds to the asymptotic limit of the SFF, $\langle K(\tau) \rangle = 1/L$, with L denoting the total number of energy levels considered. The orange dotted vertical lines mark the dip time τ_{dip} and the blue dotted vertical lines mark the Heisenberg time τ_H .

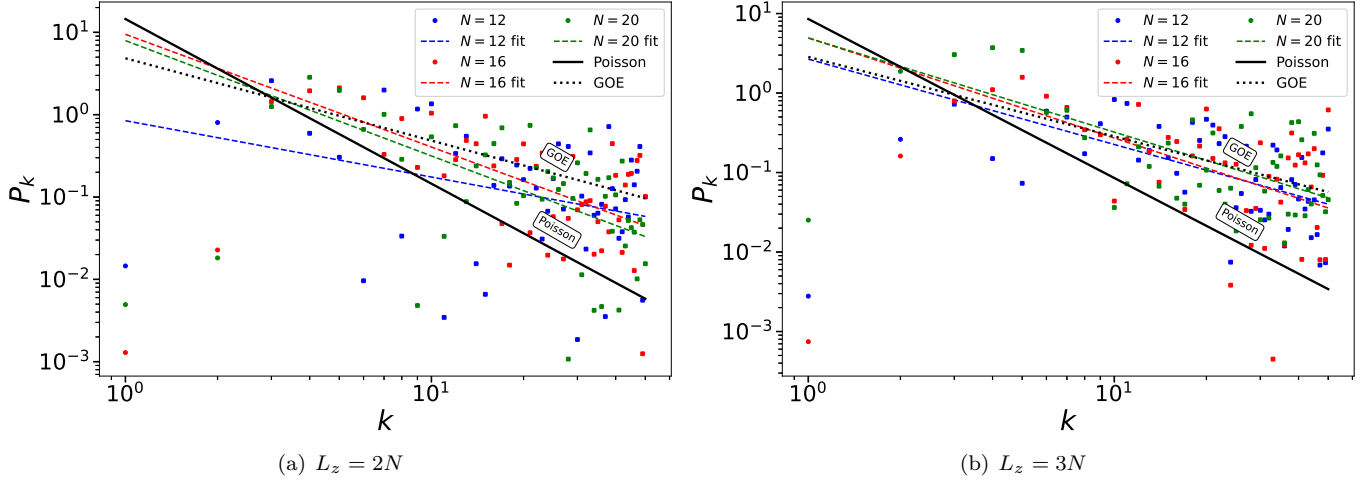


FIG. 6. (Color online) Plot of the power spectrum P_k vs k on the log-log scale in the strong interaction regime for $N = 12, 16$ and 20 bosons with total angular momentum $L_z = 2N$ (left) and $L_z = 3N$ (right). The dots are our numerical results of $N = 12, 16$ and 20 bosons. The blue dashed, the red dashed and the green dashed lines are the straight line fits for $N = 12, 16$ and 20 bosons, respectively. The black square line and the black solid line are the reference lines for the GOE and the Poisson statistics, respectively.

configurations increases. This enhancement of mode mixing strengthens the spectral correlations compared to the non-rotating case. Nevertheless, the system does not fully reach the regime described by the GOE, which is characteristic of strongly chaotic dynamics. Instead, it enters a pseudo-integrable regime—an intermediate state where the level statistics deviate from integrability but still fall short of exhibiting the universal correlations predicted by RMT for chaotic systems. This intermediate behavior is clearly reflected in the SFF. The numerical results, shown

in Fig. 3 (upper panel), reveal the development of a small but distinct linear ramp following the initial decay, eventually saturating into a plateau at longer times. The appearance of this ramp-plateau structure indicates the presence of vortex-induced correlations: the vortex introduces enough perturbation to generate partial level repulsion, but not strong enough to drive the system into full chaos. Thus, the SFF provides a direct signature of how vortex formation modify the underlying spectral properties of the condensate. This observation is further supported by the power

spectrum, where linear fits yield power-law exponents in the range $1 < \alpha < 2$. The partial breakdown of integrability and the emergence of pseudo-integrable characteristics thus clearly stem from the presence of the quantized single-vortex state in the condensate.

2. Strong interaction regime

The SFF and power spectrum for the rotating single-vortex state in the strong interaction regime are shown in Fig. 3 (lower panel) and Fig. 4 (right panel), respectively. Due to the combined effects of the quantized single vortex and the substantial condensate depletion induced by strong interactions, the SFF develops a linear ramp that is significantly more pronounced than what is observed in the moderate interaction regime. These two mechanisms work together to enhance spectral correlations in a cooperative manner. First, the strong interparticle interactions drive particles out of the macroscopically occupied ground state and into higher single-particle orbitals. This redistribution of particles reduces the condensate fraction and increases the number of accessible many-body configurations. As a larger number of particles of the system's population occupies excited states, the level structure becomes denser and more strongly mixed, thereby increasing spectral correlations. Second, the presence of a quantized single vortex further perturbs the condensate by introducing a phase winding and altering the underlying single-particle states. The vortex-induced distortion enhances coupling between modes and increases the degree of mixing among the many-body eigenstates. When combined with the interaction-driven depletion, this perturbation amplifies the deviations from integrability and pushes the system toward chaotic behavior. As a result of these two effects acting simultaneously, the system no longer resides in the pseudo-integrable regime characteristic of the moderate interaction case. Instead, it transitions into a strongly chaotic regime, where the spectral correlations resemble those predicted by RMT. This transition is clearly reflected in the SFF: the linear ramp becomes much more pronounced, especially for the case of $N = 16$, indicating a stronger degree of chaos compared to the $N = 12$ and $N = 20$ boson systems. The enhanced ramp for $N = 16$ highlights that the interplay between interactions and rotation produces the strongest chaotic signatures for this number of boson. As shown in Fig. 4 (right panel), the power-law exponents α for different number of bosons N found to be unity, further indicating that the system exhibits strong chaotic behavior. Hence, the transition to strong chaos can be attributed to the interplay between strong interaction and the quantized vortex.

C. Multi-vortex ($L_z = 2N$ and $3N$) states

The SFF and power spectrum for the multi-vortex states ($L_z = 2N$ and $3N$) in the strong interaction regime are shown in Fig. 5 (upper panel) and Fig. 6 (left panel), respectively. As a consequence of the combined influence of multiple quantized vortices and strong interparticle interactions, the SFF develops a clearly pronounced linear

ramp, which eventually saturates into a constant plateau at long times. This characteristic ramp-plateau structure is a hallmark of strong quantum chaos and indicates that the underlying energy spectrum exhibits substantial level repulsion and long-range correlations. At higher angular momenta, the system nucleates multiple quantized vortices. The presence of the vortices significantly modifies the condensate wavefunction by introducing multiple phase windings and complex flow patterns. Each vortex perturbs the single-particle states, and together they generate a highly nontrivial energy landscape. This vortex-induced perturbation enhances coupling between many-body configurations, thereby strengthening spectral correlations. Simultaneously, strong interparticle interactions scatter a considerable fraction of the particles out of the condensate and into higher excited states. This interaction-driven depletion of the BEC reduces coherence in the ground-state mode and creates a denser configuration space of accessible excited states. As particles increasingly populate these higher excited states, the many-body spectrum becomes more intricate and exhibits stronger mixing among eigenstates. The combined influence of these two mechanisms—vortex-induced structural perturbations that deplete the condensate, and interaction-driven condensate depletion—pushes the system away from integrability and firmly into a strongly chaotic regime. This transition is reflected in the SFF through the emergence of a robust linear ramp and its eventual saturation, signaling the development of spectral correlations consistent with those predicted by RMT for chaotic quantum systems. The power-law exponents α is found to approach unity for $N = 12, 16$ and 20 bosons, further indicating the onset of strong chaotic behavior in the system.

V. CONCLUSION

In summary, we have carried out an exact diagonalization study of the spectral form factor and the power spectrum for harmonically confined interacting bosons in two distinct regimes: moderate and strong interactions. Our analysis includes both non-rotating and rotating single-vortex states in the moderate and strong interaction regimes, while the multi-vortex states are examined only in the strong interaction regime.

For the non-rotating case in the moderate interaction regime, the spectral form factor (SFF) exhibits only a dip-plateau structure, with no linear ramp present. This indicates that the system predominantly retains regular behavior. Consistently, the power spectrum shows that the fitting lines for different number of bosons lie close to the Poisson statistics, with a power exponent near $\alpha \approx 2$, leading to the integrable nature of the system. In the strong interaction regime, however, a small linear ramp emerges in the SFF, signaling enhanced spectral correlations. This demonstrates that integrability is broken as the interaction strength increases, and the system transitions into a pseudo-integrable regime. The power spectrum further supports this, with power exponents falling in the range $1 < \alpha < 2$, consistent with pseudo-integrable regime.

For the rotating single-vortex state in the moderate in-

teraction regime, the SFF displays a small ramp before saturating to a plateau. This behavior arises from the formation of a quantized single-vortex in the condensate, which perturbs the system and partially breaks integrability, placing it in a pseudo-integrable regime. Correspondingly, the power spectrum yields a power-law exponent in the range $1 < \alpha < 2$, consistent with pseudo-integrable regime. In the strong interaction regime, the SFF exhibits a pronounced linear ramp followed by saturation to a plateau, reflecting the combined influence of the single-vortex state and strong interactions, which drive the system into a strongly chaotic regime. The power spectrum in this case shows a power-law exponent close to $\alpha \approx 1$, exhibiting the emergence of strong chaos. For the multi-vortex states in the strong interaction regime, the system displays pronounced chaotic behavior, resulting from the combined effects of multiple quantized vortices at higher angular momenta and strong interactions.

The SFF and power spectrum present a consistent picture, showing that condensate depletion—caused by vortex formation and strong interactions—serves as the key mechanism driving the crossover from integrable to chaotic behavior in trapped Bose systems.

ACKNOWLEDGMENTS

Mohd Talib thanks the Ministry of Social Justice and Empowerment, Government of India, for providing the Senior Research Fellowship (SRF) (*NBCFDC Ref. No.: 221610104398*).

Appendix A: Tracing out of the z-degree of freedom

From the N -body Hamiltonian in Eq. (1), the one-body non-interacting Hamiltonian for motion along the z -direction is given by

$$\hat{h}_z = \frac{1}{2M} \left(\frac{\hbar}{i} \nabla_z \right)^2 + \frac{1}{2} M \omega_z^2 z^2 \quad (\text{A1})$$

The eigensolution for $\hat{h}_z u_{n_z}(z) = (n_z + \frac{1}{2}) \hbar \omega_z u_{n_z}(z)$ with $n_z = 0, 1, 2, \dots$, is given by

$$u_{n_z}(z) = \sqrt{\frac{\alpha_z}{\sqrt{\pi} 2^{n_z} n_z!}} e^{-\frac{1}{2} \alpha_z^2 z^2} H_{n_z}(\alpha_z z), \quad (\text{A2})$$

where $\alpha_z \equiv \sqrt{\frac{M \omega_z}{\hbar}}$ and $H_{n_z}(\alpha_z z)$ is a Hermite polynomial. The effective Hamiltonian in xy -plane obtained by tracing out the z -degree of freedom for the Hamiltonian in Eq. (1) as

$$\hat{H}' = \langle u_{n_z}(z) | \hat{H}^{\text{lab}} | u_{n_z}(z) \rangle \quad (\text{A3})$$

is given, for $n_z = 0$, by

$$\begin{aligned} \hat{H}' = & \sum_{i=1}^N \left[\frac{1}{2M} \left(\frac{\hbar}{i} \nabla_{\perp i} \right)^2 + \frac{1}{2} M \omega_{\perp}^2 r_{\perp i}^2 \right] \\ & + \frac{1}{2} \hbar \omega_z \\ & + \frac{4\pi \hbar^2 a_{sc}}{M} \frac{1}{\sqrt{2\pi}} \sqrt{\frac{\lambda_z}{a_{\perp}^2 \left[1 + \left(\frac{\sigma}{a_{\perp}} \right)^2 \lambda_z \right]}} \\ & \times \left(\frac{1}{\sqrt{2\pi} \sigma} \right)^2 \sum_{i \neq j}^N \exp \left[-\frac{(r_{\perp i} - r_{\perp j})^2}{2\sigma^2} \right]. \end{aligned} \quad (\text{A4})$$

-
- [1] M. V. Berry and M. Tabor, Level clustering in the regular spectrum, *Proc. R. Soc. Lond. A* **356**, 375 (1977).
 - [2] O. Bohigas, M. J. Giannoni, and C. Schmit, Characterization of Chaotic Quantum Spectra and Universality of Level Fluctuation Laws, *Phys. Rev. Lett.* **52**, 1 (1984).
 - [3] F. J. Dyson, Statistical Theory of the Energy Levels of Complex Systems. I, *Journal of Mathematical Physics* **3**, 140 (1962).
 - [4] F. J. Dyson, The Threefold Way. Algebraic Structure of Symmetry Groups and Ensembles in Quantum Mechanics, *Journal of Mathematical Physics* **3**, 1199 (1962).
 - [5] M. Talib and M. A. H. Ahsan, Exact diagonalization study of energy level statistics in harmonically confined interacting bosons, *arXiv preprint arXiv:2508.01729* (2025).
 - [6] A. Chan, A. De Luca, and J. T. Chalker, Solution of a minimal model for many-body quantum chaos, *Phys. Rev. X* **8**, 041019 (2018).
 - [7] P. Kos, M. Ljubotina, and T. Prosen, Many-Body Quantum Chaos: Analytic Connection to Random Matrix Theory, *Phys. Rev. X* **8**, 021062 (2018).
 - [8] B. Bertini, P. Kos, and T. Prosen, Exact spectral form factor in a minimal model of many-body quantum chaos, *Phys. Rev. Lett.* **121**, 264101 (2018).
 - [9] A. K. Das, C. Cianci, D. G. A. Cabral, D. A. Zarate-Herrada, P. Pinney, S. Pilatowsky-Cameo, A. S. Matsoukas-Roubas, V. S. Batista, A. del Campo, E. J. Torres-Herrera, and L. F. Santos, Proposal for many-body quantum chaos detection, *Phys. Rev. Res.* **7**, 013181 (2025).
 - [10] E. Cáceres, A. Misobuchi, and A. Raz, Spectral form factor in sparse SYK models, *Journal of High Energy Physics* **2022**, 1 (2022).
 - [11] P. Orman, H. Gharibyan, and J. Preskill, Quantum chaos in the sparse SYK model, *Journal of High Energy Physics* **2025**, 1 (2025).
 - [12] J. S. Cotler, G. Gur-Ari, M. Hanada, J. Polchinski, P. Saad, S. H. Shenker, D. Stanford, A. Streicher, and M. Tezuka, Black holes and random matrices, *Journal of High Energy Physics* **2017**, 1 (2017).
 - [13] A. M. García-García and J. J. M. Verbaarschot, Spectral and thermodynamic properties of the Sachdev-Ye-Kitaev model, *Phys. Rev. D* **94**, 126010 (2016).
 - [14] P. Saad, S. H. Shenker, and D. Stanford, A semiclassical ramp in SYK and in gravity, *arXiv preprint arXiv:1806.06840* (2018).

- [15] J. Liu, Spectral form factors and late time quantum chaos, *Phys. Rev. D* **98**, 086026 (2018).
- [16] J. Šuntajs, J. Bonča, T. Prosen, and L. Vidmar, Quantum chaos challenges many-body localization, *Phys. Rev. E* **102**, 062144 (2020).
- [17] A. Prakash, J. H. Pixley, and M. Kulkarni, Universal spectral form factor for many-body localization, *Phys. Rev. Res.* **3**, L012019 (2021).
- [18] S. J. Garratt and J. T. Chalker, Many-body delocalization as symmetry breaking, *Phys. Rev. Lett.* **127**, 026802 (2021).
- [19] H. Dong, P. Zhang, C. B. Dağ, Y. Gao, N. Wang, J. Deng, X. Zhang, J. Chen, S. Xu, K. Wang, Y. Wu, C. Zhang, F. Jin, X. Zhu, A. Zhang, Y. Zou, Z. Tan, Z. Cui, Z. Zhu, F. Shen, T. Li, J. Zhong, Z. Bao, H. Li, Z. Wang, Q. Guo, C. Song, F. Liu, A. Chan, L. Ying, and H. Wang, Measuring the Spectral Form Factor in Many-Body Chaotic and Localized Phases of Quantum Processors, *Phys. Rev. Lett.* **134**, 010402 (2025).
- [20] A. Relaño, J. M. G. Gómez, R. A. Molina, J. Retamosa, and E. Faleiro, Quantum chaos and $1/f$ noise, *Phys. Rev. Lett.* **89**, 244102 (2002).
- [21] E. Faleiro, J. M. G. Gómez, R. A. Molina, L. Muñoz, A. Relaño, and J. Retamosa, Theoretical derivation of $1/f$ noise in quantum chaos, *Phys. Rev. Lett.* **93**, 244101 (2004).
- [22] A. Relaño, Chaos-assisted tunneling and $1/f^\alpha$ spectral fluctuations in the order-chaos transition, *Phys. Rev. Lett.* **100**, 224101 (2008).
- [23] J. M. G. Gómez, A. Relaño, J. Retamosa, E. Faleiro, L. Salasnich, M. Vraničar, and M. Robnik, $1/f^\alpha$ noise in spectral fluctuations of quantum systems, *Phys. Rev. Lett.* **94**, 084101 (2005).
- [24] A. Relaño, J. Retamosa, E. Faleiro, R. A. Molina, and A. P. Zuker, $1/f$ noise and very high spectral rigidity, *Phys. Rev. E* **73**, 026204 (2006).
- [25] M. S. Santhanam and J. N. Bandyopadhyay, Spectral fluctuations and $1/f$ noise in the order-chaos transition regime, *Phys. Rev. Lett.* **95**, 114101 (2005).
- [26] J. Mur-Petit and R. A. Molina, Spectral statistics of molecular resonances in erbium isotopes: How chaotic are they?, *Phys. Rev. E* **92**, 042906 (2015).
- [27] M. H. Anderson, J. R. Ensher, M. R. Matthews, C. E. Wieman, and E. A. Cornell, Observation of Bose-Einstein Condensation in a Dilute Atomic Vapor, *Science* **269**, 198 (1995).
- [28] M. A. H. Ahsan and N. Kumar, Rotating Bose gas with hard-core repulsion in a quasi-two-dimensional harmonic trap: Vortices in Bose-Einstein condensates, *Phys. Rev. A* **64**, 013608 (2001).
- [29] M. Imran and M. A. H. Ahsan, Vortex patterns in moderately rotating Bose-condensed gas, *J. Phys. B: At. Mol. Opt. Phys.* **50**, 045301 (2017).
- [30] M. Imran and M. A. H. Ahsan, Novel phases in rotating Bose-condensed gas: vortices and quantum correlation, *The European Physical Journal D* **77**, 79 (2023).
- [31] E. J. Mueller, T.-L. Ho, M. Ueda, and G. Baym, Fragmentation of Bose-Einstein condensates, *Phys. Rev. A* **74**, 033612 (2006).
- [32] A. Tomadin, S. Diehl, and P. Zoller, Nonequilibrium phase diagram of a driven and dissipative many-body system, *Phys. Rev. A* **83**, 013611 (2011).
- [33] S. Inouye, M. R. Andrews, J. Stenger, H.-J. Miesner, D. M. Stamper-Kurn and W. Ketterle, Observation of Feshbach resonances in a Bose-Einstein condensate, *Nature* **392**, 151 (1998).
- [34] C. Chin, R. Grimm, P. Julienne and E. Tiesinga, Feshbach resonances in ultracold gases, *Rev. Mod. Phys.* **82**, 1225 (2010).
- [35] E. R. Davidson, The iterative calculation of a few of the lowest eigenvalues and corresponding eigenvectors of large real-symmetric matrices, *Journal of Computational Physics* **17**, 87 (1975).
- [36] M. L. Mehta, *Random Matrices* (Academic Press, New York, 1991).
- [37] H.-J. Stöckmann, *Quantum Chaos: An Introduction* (Cambridge University Press, Cambridge, 2000).
- [38] F. Haake, *Quantum Signatures of Chaos* (Springer-Verlag, Berlin, 2010).
- [39] Y.-N. Zhou, T.-G. Zhou, and P. Zhang, General properties of the spectral form factor in open quantum systems, *Frontiers of Physics* **19**, 10.1007/s11467-024-1406-7 (2024).
- [40] R. E. Prange, The Spectral Form Factor Is Not Self-Averaging, *Phys. Rev. Lett.* **78**, 2280 (1997).
- [41] A. K. Das, A. Ghosh, and L. F. Santos, Spectral form factor and energy correlations in banded random matrices, *Phys. Rev. B* **111**, 224202 (2025).
- [42] R. Riser, V. A. Osipov, and E. Kanzieper, Power spectrum of long eigenlevel sequences in quantum chaotic systems, *Phys. Rev. Lett.* **118**, 204101 (2017).
- [43] F. Dalfovo and S. Stringari, Bosons in anisotropic traps: Ground state and vortices, *Phys. Rev. A* **53**, 2477 (1996).
- [44] G. Baym and C. J. Pethick, Ground-State Properties of Magnetically Trapped Bose-Condensed Rubidium Gas, *Phys. Rev. Lett.* **76**, 6 (1996).
- [45] F. Dalfovo, S. Giorgini, L. P. Pitaevskii and S. Stringari, Theory of Bose-Einstein condensation in trapped gases, *Rev. Mod. Phys.* **71**, 463 (1999).
- [46] M. Arazo Sánchez, *Anisotropic interactions and self-bound solutions in Bose-Einstein condensates*, Ph.D. thesis (2024).